CHEMISTRY
A EUROPEAN JOURNAL

FULL PAPER

DOI: 10.1002/chem.201203625

Synthesis of Luminescent Ethynyl-Extended Regioisomers of Borate Complexes Based on 2-(2′-Hydroxyphenyl)benzoxazole

Julien Massue,*[a] Denis Frath,[a] Pascal Retailleau,[b] Gilles Ulrich,*[a] and Raymond Ziessel*[a]

Abstract: A series of thirteen luminescent tetrahedral borate complexes based on the 2-(2′-hydroxyphenyl)-benzoxazole (HBO) core is presented. Their synthesis includes the incorporation of an ethynyl fragment by Sonogashira cross-coupling reaction, with the goal of extending the conjugation and consequently redshifting their emission wavelength. Different regioisomers, substituted in the 3-, 4-, or 5-position of the phenolate side of the HBO core, were studied in order to compare their photophysical properties. The complexes were characterized by X-ray diffraction and NMR, UV/Vis, and emission spectroscopy in solution and in the solid state. In all cases, complexation to boron leads to a donor–acceptor character that impacts their photophysical properties. Complexes with a 3- or 5-substituted fragment display mild to pronounced internal charge transfer (ICT), a feature strengthened by the presence of *p*-dibutylaminophenylacetylene in the molecular structure, protonation of the nitrogen atom of which leads to a significant blueshift and an increase in quantum yield. On the contrary, when the ethynyl module is grafted on the 4-position, narrow, structured, symmetrical absorption/emission bands are observed. Moreover, the fact that protonation has little effect on the emission maximum wavelength reveals singlet excited-state decay. Solid-state emission properties reveal a redshift compared to solution, explained by tight packing of the π-conjugated systems and the high planarity of the dyes. Subsequent connection of these complexes to other photoactive subunits (BODIPY, Boranil) provides dyads in which efficient cascade energy transfer is observed.

Keywords: alkynes · borates · dyes/pigments · heterocycles · luminescence

Introduction

Organic fluorescent dyes have become indispensable tools for chemists and biologists in a broad range of technologies ranging from imaging, medical diagnosis, and photodynamic therapy[1] to organic electronics and solar-energy conversion.[2] For example, their unique ability to absorb photons of light at a given wavelength and to re-emit lower-energy light has proved to be extremely useful in medical imaging, where these dyes are commonly used to help visualize various biological events occurring in organs, tissues, or cells. Owing to fine-tuning of their luminescence properties due to microchanges in their environment, they have found interest as sensors for biological materials, toxins, and wastes[3] and in bioconjugation to proteins,[4] oligosaccharides,[5] synthetic polymers,[6] nanoparticles,[7] and carbon nanotubes.[8] Coumarins,[9] fluoresceins,[10] cyanines,[11] Rhodamines,[12] squaraines,[13] and boron dipyrromethene (BODIPY) dyes[3b,14] are currently among the most popular families of dyes. They have gained their tremendous popularity because they meet most of the requirements for organic dyes: sharp and narrow absorption and fluorescence emission spectra, chemical and photostability, high absorption coefficients, high quantum yields, and good solubility. Moreover, there is the possibility to fine-tune their maximum emission wavelength by introducing functional groups and/or extending the conjugation around the fluorescent core. The drawback of these dyes is that they often exhibit small Stokes shifts, especially in the case of BODIPY dyes, due to minimal reorganization of the molecules on photoexcitation. One strategy to increase the Stokes shifts is to desymmetrize the molecular structure of the boron-containing dye. Unlike the dipyrrin core present in BODIPY, unsymmetrical structures would indeed be more prone to have energetically separated ground and excited states and therefore larger Stokes shifts.[15]

There is increasing interest in solid-state emitters, which are key materials in a wide range of technologies including luminescent sensors, telecommunications, and lasers.[16]

[a] Dr. J. Massue, D. Frath, Dr. G. Ulrich, Dr. R. Ziessel
Laboratoire de Chimie Moléculaire et
Spectroscopies Avancées (LCOSA)
ICEEPS–LCOSA, UMR CNRS 7515
École Européenne de Chimie, Polymères et Matériaux (ECPM)
25 rue Becquerel, 67087 Strasbourg Cedex 02 (France)
Fax: (+33) 3-68-85-27-6
E-mail: massue@unistra.fr
gulrich@unistra.fr
ziessel@unistra.fr
Homepage: http://www-lmspc.u-strasbg.fr/lcosa

[b] P. Retailleau
Laboratoire de Cristallochimie, ICSN–CNRS
Bât 27-1 avenue de la Terrasse, 91198 Gif-sur-Yvette, Cedex (France)

Supporting information for this article is available on the WWW under http://dx.doi.org/10.1002/chem.201203625.

Solid-state luminescence is usually observed for dyes that are decorated with peripheral bulky substituents to prevent concentration annihilation caused by intermolecular interactions.[17] The search for new bright, stable, scalable, and red-emitting dyes being endless due to the growing demand for novel structures, it is imperative to design and investigate the properties of other types of fluorescent dyes with original molecular structures and improved photophysical properties, both in solution and in the solid state. Coordination of a π-conjugated ligand to a boron(III) center (e.g., BF_2, BPh_2) rigidifies the molecule, which leads to high fluorescence yields with larger Stokes shifts than observed in BODIPY dyes.[18] Different ways to modulate their optical and electronic properties have been explored.

The structural and photophysical properties of different families of boron complexes have been reported in the literature, among which neutral, coordinately saturated, N,N (excluding BODIPYs),[15,19] N,N,O,O tetradentate,[20] O,N,O tridentate,[21] and N,O bidentate ligands have been described. The N,O chelating ligands are by far the most studied π-conjugated ligands, including a wide range of structures with single or multiple boron centers, mainly as hydroxyquinolate,[22] pyrene,[23] perylenetetracarboxylic diimides (PDIs),[24] and Schiff bases,[25] but some more exotic structures such as iminoketone[26] and azaoxobenzazulene[27] have also been reported.

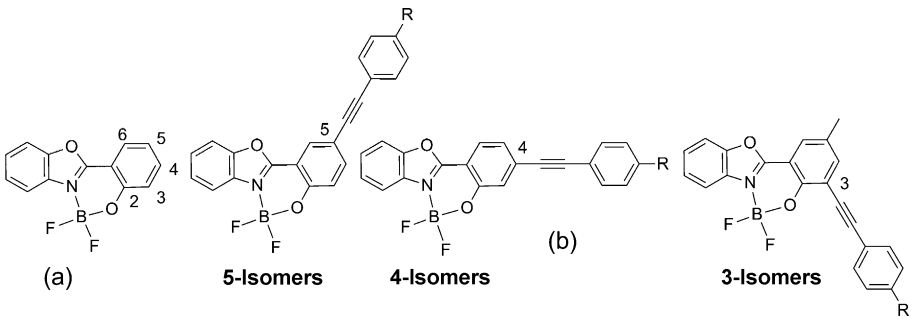

Scheme 1. a) 2-(2′-Hydroxyphenyl)benzoxazole borate complex. b) General structure of the compounds studied in this work.

Abstract in French: *Cet article présente une série de treize complexes de bore tétraédriques luminescents basés sur le motif 2-(2′-hydroxyphenyl)benzoxazole (HBO). Leur synthèse comprend l'incorporation d'un fragment ethynyle par une réaction de couplage croisé de Sonogashira dans le but d'étendre la conjugaison et ainsi déplacer leur longueur d'onde d'émission dans le rouge (basses longueur d'onde). Différents régioisomères, substitués en position 3, 4 ou 5 du côté phénol du groupement HBO ont été étudiés afin de comparer leurs propriétés spectroscopiques. Les complexes ont été caractérisés par RMN, diffraction des rayons X sur monocrystal, spectroscopie UV-Visible et émission à la fois en solution et à l'état solide. Pour chaque composé, la complexation au bore entraine un caractère donneur-accepteur de la molécule, ce va qui fortement influer sur les propriétés photophysiques. Les complexes fonctionnalisés en position 3 et 5 présentent un transfert de charge interne (TCI) qui est amplifié par la présence du groupement dibutylaminophénylacetylène dans la structure des molécules; la protonation de l'atome d'azote par de l'HCl gazeux entraine un déplacement de la longueur d'onde d'émission vers le bleu (longueur d'onde plus élevée) et une augmentation du rendement quantique. A l'opposé, lorsque l'espaceur éthynyle est greffé en position 4, des bandes d'absorption/émission étroites, structurées et symétriques sont observées. Par ailleurs, la protonation n'a que peu d'effet sur le maximum de la longueur d'onde d'émission, mettant en évidence une décroissance de l'état excité de type singulet. L'étude des propriétés d'émission à l'état solide révèlent un déplacement vers le rouge en comparaison des propriétés en solution, qui est expliqué par les empilements importants des systèmes conjugués et la grande planéité des colorants. La connexion de ces complexes à d'autres sous-unités photoactives (BODIPY, Boranil) permet d'obtenir des dyades où un transfert d'énergie en cascade est observé.*

Following a pioneer paper,[28] we recently presented the synthesis of 2-(2′-hydroxyphenyl)benzoxazole (HBO) derivatives coordinated to a BF_2 fragment (Scheme 1a).[29] These dyes are very stable in solution in nonpolar solvents and show bright fluorescence and improved Stokes shifts. Their emission is mostly located in the UV part of the spectrum, with maximum emission wavelengths ranging from 385 to 425 nm in toluene. However, these high-energy emissions impede all kind of in vivo applications due to the high absorption of biological backgrounds in the UV region.

Furthermore, unsubstituted HBO/HBT borate complex dyes are poorly soluble in polar solvents such as water, alcohols, and DMSO, in which they also undergo boron decomplexation. A few requirements must be fulfilled to improve the stability and redshift the emission of the dyes: 1) increase the electronic density on the phenolic side of the HBO core, as a prerequisite for improving the chemical stability in polar, protic solvents, in which the B–O bond is prone to hydrolysis; 2) extension of the conjugation to increase the delocalization and therefore lower the LUMO level of the molecule and consequently bathochromically shift the fluorescence emission. A few recent papers discuss the direct influence of dialkyl- and diarylamino groups at the 5- and 4-positions of the HBO core.[30] However, the photophysical effects of further extending the conjugation and of substituents at the 3-position of the HBO core have not been studied.

Here we report on our synthetic efforts to redshift the emission wavelength and improve both the Stokes shifts and the stability of HBO borate complexes. Our goal was to prepare and characterize three different families of regioisomers with various electron-donating or electron-withdrawing groups in order to compare their photophysical features. Synthesis of the dyes includes connection of a decorated phenylacetylene fragment to the phenolic side of the HBO core in the 3-, 4-, or 5-position (Scheme 1b). All compounds of interest were prepared by Pd-catalyzed Sonogashira cross-coupling reactions with an appropriate acetylene fragment.

The influence of 1) the electronic nature of the extended fragment and 2) its position on the phenol ring of the HBO core (3, 4, or 5) on the photophysical properties were scrutinized. Finally, we showed that Sonogashira cross-coupling reactions allow the attachment of these new dyes to photoactive subunits such as BODIPY or Boranil[31] cores to give sophisticated molecular cassettes.

Results and Discussion

Synthetic strategies and preparation of the 5-, 4-, and 3-substituted regioisomers of 2-(2′-hydroxyphenyl)benzoxazole (HBO) borate complexes are summarized in Schemes 2–4.

Selective mono-iodination of commercially available salicylaldehyde and 4-methoxysalicylaldehyde with an excess of iodine monochloride in acetic acid leads to 5-iodosalicylaldehydes **1** and **2** in good yields (Scheme 2). The other iodo regioisomers were not observed when the reaction was performed at room temperature. 5-Iodosalicylaldehydes **1** and **2** were then condensed with one equivalent of 2-aminophenol in refluxing ethanol to yield a cyclic carbinolamine, which underwent oxidative cyclization with 2,3-dichloro-5,6-dicyano-1,4-benzoquinone (DDQ) in dichloromethane at room temperature. Purification by column chromatography afforded 5-iodo HBOs **3** and **4** in 87 and 63% yield respectively. These compounds exhibit strong blue-green fluorescence in the solid state due to an excited-state intramolecular proton transfer (ESIPT),[32] as evidenced by a distinctive downfield ^{1}H NMR signal for the strongly H-bonded phenolic proton around 11 ppm. Compounds **3** and **4** were then subjected to Sonogashira cross-coupling reaction conditions. The optimal protocol was found to involve the use of 5% $[PdCl_2(PPh_3)_2]$ catalyst and 10% copper iodide in the presence of triethylamine as base in toluene at room temperature overnight. These reaction conditions allowed facile introduction of various acetylene modules at the 5-position of the phenolic side of the HBO core with yields ranging from 29 to 93% for **5**–**10** (Scheme 2). Introduction of a methoxy group at the 4-position of the HBO core, as in **9** and **10**, was carried out with the aim of further increasing the electron density on the phenolic side of the HBO and hence the stability of the corresponding HBO borate complexes. Dropwise addition of $BF_3{\cdot}Et_2O$ to a solution of HBO ligands **5**–**10** in anhydrous dichloromethane at room temperature in the presence of *N*,*N*-diisopropylethylamine (DIEA) as base allowed straightforward boron complexation at the N,O chelating site. Pure complexes **11**–**16** were obtained after purification by filtration through a basic Al_2O_3 column, eluted with CH_2Cl_2. All compounds were characterized by ^{1}H, ^{13}C, and ^{11}B NMR as well as MS and elemental analysis.

The synthesis of the 4-substituted HBO borate complexes is described in Scheme 3. 4-Iodosalicylaldehyde (**17**) was obtained by monoformylation of 3-iodophenol with paraformaldehyde in anhydrous THF in 28% yield. 6-Iodosalicylaldehyde is also formed as a side product in the course of the reaction but easily separated by column chromatography. Condensation of **17** with 2-aminophenol in refluxing ethanol followed by oxidative cyclization with DDQ afforded 4-iodo HBO **18** in 80% yield. Compound **18** was then subjected to Sonogashira cross-coupling conditions similar to those used to prepare compounds **5**–**10** in the presence of *p*-tolylacetylene or *p*-dibutylaminophenylacetylene.

The HBO ligands **19** and **20** were obtained as yellow powders in 82 and 75% yield respectively. Finally, boron complexation was achieved by using similar reaction conditions as for complexes **11**–**16** (excess of

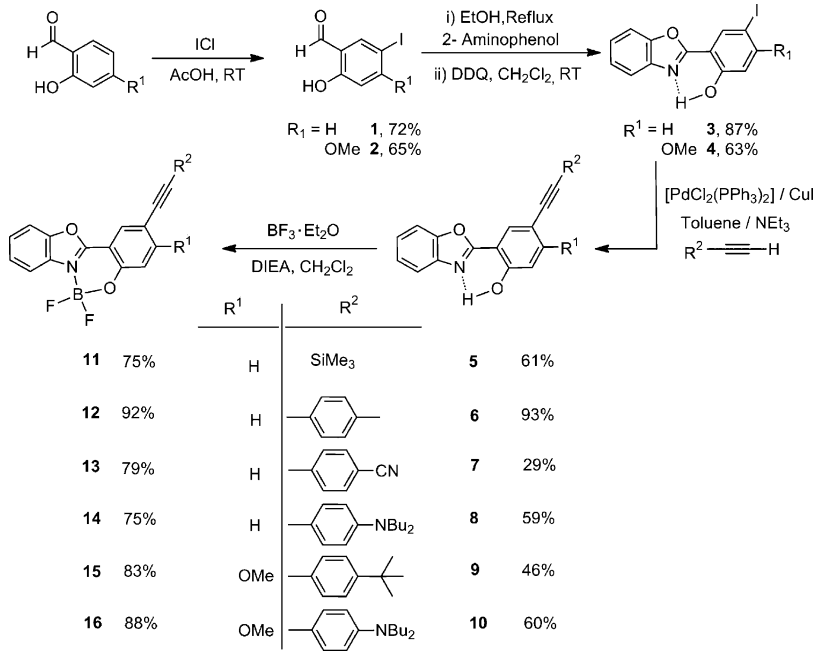

Scheme 2. Synthesis of HBO borate complexes **11**–**16**.

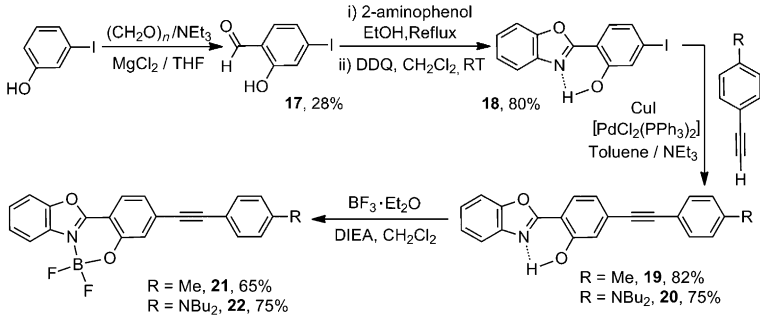

Scheme 3. Synthesis of HBO borate complexes **21** and **22**.

BF_3•Et_2O in the presence of DIEA in CH_2Cl_2). Formation of HBO ligands **19** and **20** and the corresponding BF_2 complexes **21** and **22** was monitored by ^{1}H NMR spectroscopy, whereby the downfield signal attributed to the H-bonded phenolic proton disappears on complexation (Figure 1).

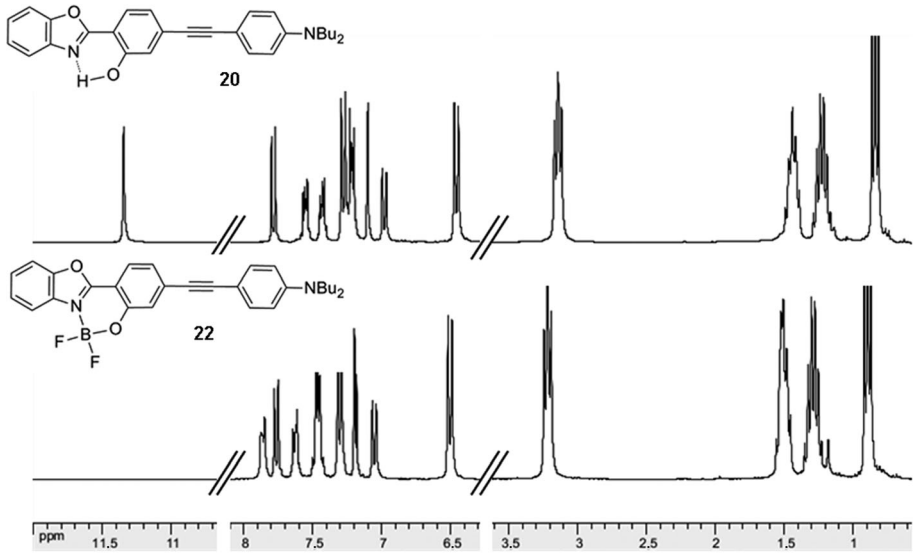

Figure 1. ^{1}H NMR spectra in $CDCl_3$ of HBO **20** and corresponding BF_2 complex **22**.

Synthesis of the 3-substituted HBO borate complexes is described in Scheme 4. Selective mono-iodination at the 3-position was achieved by using an excess of iodine monochloride on 5-methylsalicylaldehyde in acetic acid (59% yield of isolated product). 3-Iodo-5-methylsalicylaldehyde (**23**) was then condensed with 2-aminophenol and the intermediate further oxidized in the presence of DDQ to provide HBO **24** in 64% yield. To avoid in situ intramolecular nucleophilic addition of the phenolate to the triple bond under the Sonogashira cross-coupling reaction conditions (Pd^{II}, CuI, NEt_3),[33] HBO **24** was first protected with an acetate group by reaction with acetic anhydride in dichloromethane with catalytic amounts of pyridine. The crude material was immediately subjected to Sonogashira conditions with *p*-tolylacetylene or *p*-dibutylaminoacetylene as acetylene sources to yield acetate-protected HBOs **25** and **26** in 91 and 66% yield, respectively. Removal of the acetate protecting group with an excess of K_2CO_3 in MeOH/THF (1/1) provided HBOs **27** and **28** in a nearly quantitative yield. Finally, boron complexation was achieved by using an excess of BF_3•Et_2O/DIEA, and the resulting crude complexes were purified by filtration through basic Al_2O_3 to afford borate complexes **29** and **30** in 88 and 71% yield, respectively. The X-ray structure of complex **29** further confirmed connection of the phenylacetylene fragment at the 3-position of the HBO core (see below). It is noteworthy that all extended complexes exhibit improved chemical stability in protic solvents compared to reported unsubstituted ones.[29]

Finally, we investigated the effect of covalent connection of HBO borate complexes to other photoactive subunits such as BODIPY or Boranil. The synthesis of dyads **33** and **36** is

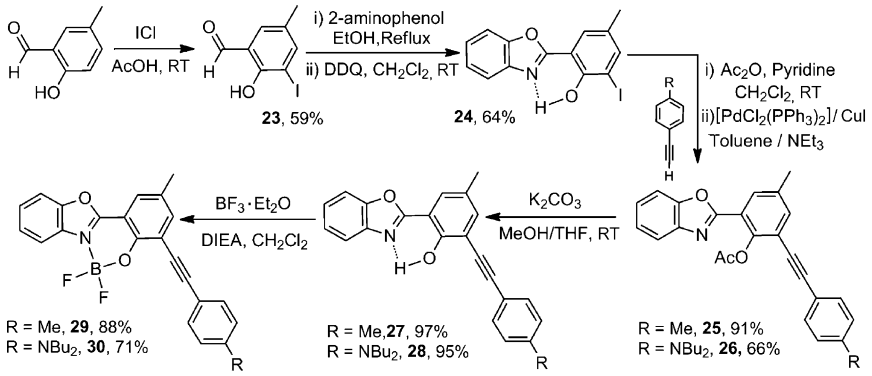

Scheme 4. Synthesis of HBO borate complexes **29** and **30**.

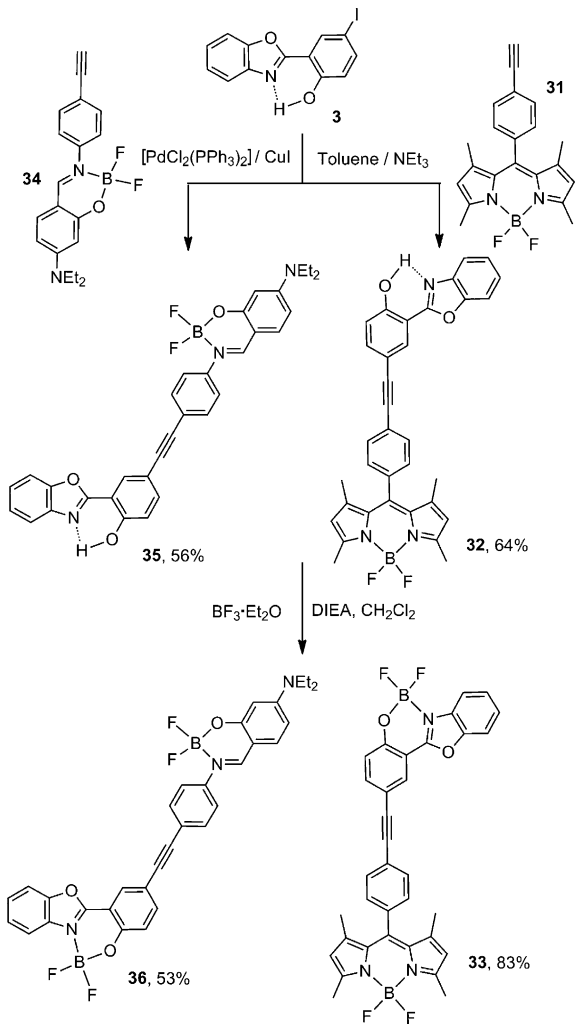

Scheme 5. Synthesis of BODIPY–HBO borate dyad **33** and Boranil–HBO borate dyad **36**.

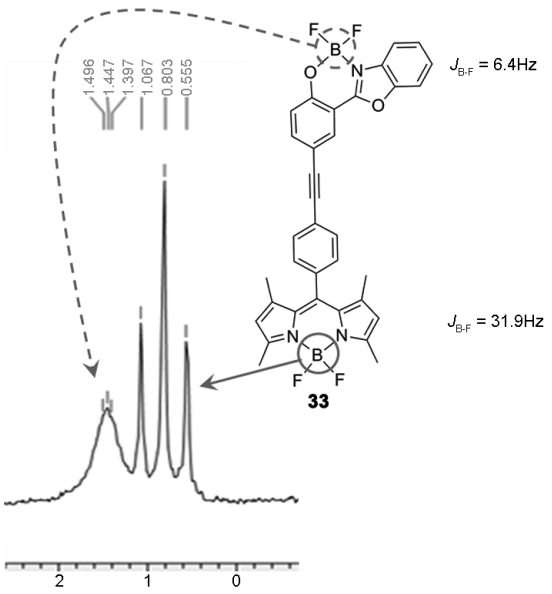

Figure 2. ^{11}B NMR spectrum of dyad **33** in $CDCl_3$ at 128.38 MHz.

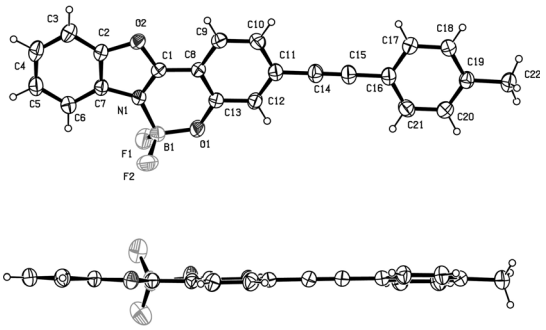

Figure 3. Top: ORTEP diagram of **21** showing the atom-labeling scheme. Bottom: View orthogonal to the above diagram to highlight the planarity of the molecule. Thermal ellipsoids are plotted at the 30% level. Bond lengths [Å] and angles [°]: B1−N1 1.581(2), B1−O1 1.442(3), B1−F1 1.363(3), B1−F2 1.367(3), N1−C1 1.307(2), N1−C7 1.405(2) Å; N-B-O 108.27(16), F-B-F 110.91(18), N-B-F 108.27(17)/108.05(16), O-B-F 109.94(17)/111.30(17).

presented in Scheme 5. Iodo HBO **3** was treated under Sonogashira cross-coupling reaction conditions (5% Pd^{II}, 10% CuI, NEt_3) in toluene with ethynyl BODIPY derivative **31** to give BODIPY **32** in 64% yield or ethynyl Boranil **34** to give dyad **35** in 56% yield. Addition of BF_3•Et_2O in the presence of DIEA in dichloromethane yielded BODIPY–HBO borate dyads **33** and Boranil–HBO borate **36** in 83 and 53% respectively. In dyad **33**, the complexation reaction can be monitored by the appearance of two triplets at 1.45 and 0.80 ppm in the ^{11}B NMR spectrum due to the coupling of the boron centers with two equivalent fluorine nuclei. The coupling constant of the HBO borate complex (J_{B-F}= 6.4 Hz) is much smaller than that of the BODIPY (J_{B-F}= 31.9 Hz) (Figure 2).

X-ray structures: Single crystals of complexes **21** and **29** suitable for X-ray analysis were obtained. The molecular structures are shown in Figures 3 and 4, respectively. Substitution of the ethynylmethylbenzene moiety at the C11 position in HBO borate complex **21** or at C12 for **29** with a methyl group at C10 does not affect the planarity of the molecule. A very small root mean squared deviation of the HBO platform (0.038 Å for 17 atoms within the heterotetracycle in **21** vs. 0.033 Å for 18 atoms in **29**) and a very small atom deviation (0.099 Å for the boron atom in **29** are the most noticeable features. The dihedral angle with the tolyl group is similar in both complexes [6.26 Å (**21**) vs. 6.46° (**29**)]. The boron center displays a fairly regular tetrahedral geometry with angles ranging from 108.2(2) to 111.3 (2)° for **21** and from 107.7(2) to 111.1 (2)° for **29**. These features are similar to some previously reported for non-extended HBO borate complexes.[29] The B1−O1 and B1−N1 distances are in the same range for **21** and **29** (1.444 vs. 1.440 Å for B1−O1 and 1.581 vs. 1.579 Å for B1−N1) and are fairly similar to those in HBO borate complexes reported in the literature.[29]

The arrangement of planar, elongated complex **21**, which crystallized in triclinic space group $P\bar{1}$, is strongly governed

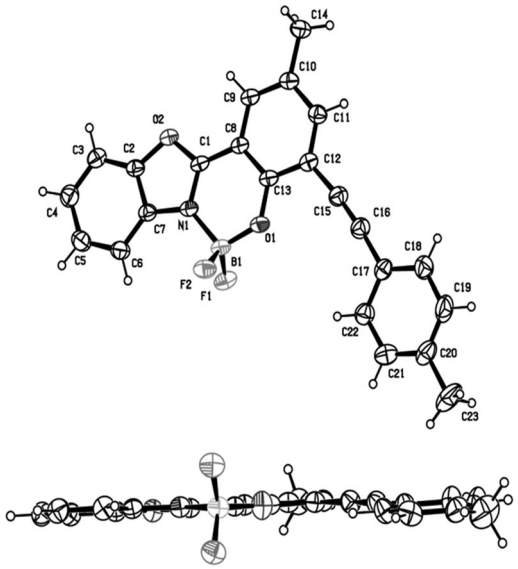

Figure 4. Top: ORTEP diagram of **29** showing the atom-labeling scheme. Bottom: View orthogonal to the above diagram highlighting the planarity of the molecule. Thermal ellipsoids are plotted at the 30% level. Bond lengths [Å] and angles [°]: B1–N1 1.579(2), B1–O1 1.440(3), B1–F1 1.377(2), B1–F2 1.370(2), N1–C1 1.319(2), N1–C7 1.399(2); N-B-O 108.58(13), F-B-F 109.43(14), N-B-F 107.74(15)/108.74(15), O-B-F 111.19(16)/111.06(16)°.

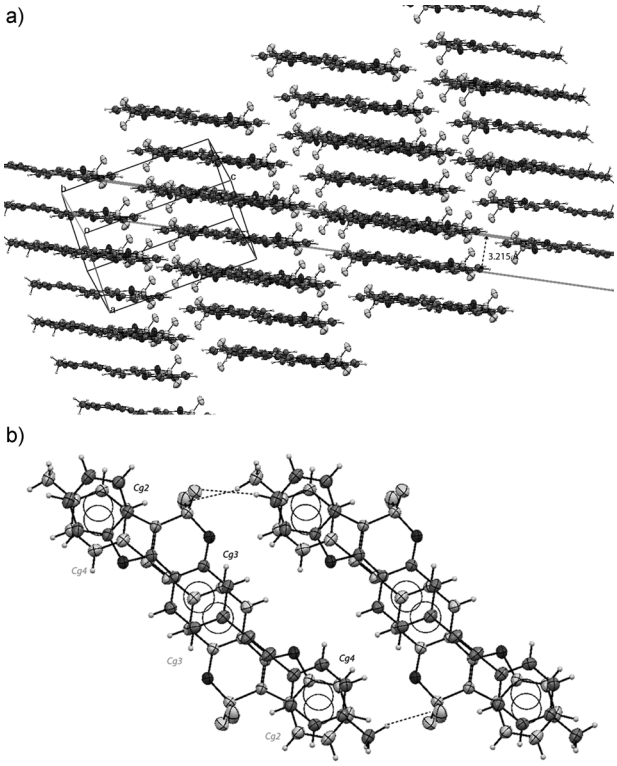

Figure 5. a) A view showing the layered crystal structure of compound **21**. b) Perpendicular view to the $(\bar{2}12)$ plane showing dimeric association in layers (CH···F interactions as dotted lines) and through π–π columnar stacking in the crystal structure of compound **21**.

by π–π stacking interactions. The molecules, all oriented along the [221] direction, lie in the $(\bar{2}12)$ plane with a tilt of 10.5°, and interact side by side through methyl and aryl hydrogen and fluorine atoms (C–H···F distances of 2.57 and 2.71 Å respectively; Figure 5a). The average interlayer distance is rather short (3.215 Å) and stacking overlap between inverted head-to-tail molecules is rather high with centroid–centroid distances between overlapping phenyl groups of about 3.72 Å (Figure 5b).

Complex **21** is also arranged in layers, which are parallel to the (123) plane with a short interlayer distance of 3.181 Å (Figure 6a). Within a layer, the L-shaped molecules form square dimers around a center of inversion held together by mutual nonclassical C6–H···F2^{i} hydrogen bonds with an H–F distance of 2.46 Å and bordered by adjacent methyl or aryl groups (see Figure 6b). Along the *b* crystallographic axis, the molecules develop strong π–π stacking interactions with infinite columns of the benzyl groups at the origin of the unit cell, the centroid–centroid distances of which vary around 4.0 Å, on one side and columns of the tetracycles at the center of the unit cell, with shortest centroid–centroid distance of 3.548 (2) Å between the pentagon at *x*,*y*,*z* and the C8–C13 six-membered ring at $1-x,-y,1-z$ on the other side (Figure 6b).

Photophysical properties: Photophysical data in various solvents for dyes **11**–**16**, **21**, **22**, **29**, **30**, **32**, **33**, and **36** are listed in Table 1. Absorption and emission properties of complex **16** in various solvents are presented in Figure 7, and a comparison of the regioisomers containing a *p*-tolylacetylene fragment (**12**, **21**, **29**) is shown in Figure 8. Spectra of dyes containing a *p*-dibutylaminophenylacetylene group (**14**, **16**, **22**, **30**) are shown in Figure 9.

As a general trend, all HBO borate complexes except **21** exhibit rather similar absorption spectra with an unstructured, large absorption band between 342 and 401 nm and extinction coefficients in the range 8000–48000 $M^{-1}cm^{-1}$, depending on the electronic substitution on the phenyl core. More intense bands are observed below 300 nm, characteristic of the π–π* transitions of the phenyl rings. A noteworthy exception is dye **21**, for which a structured, narrow absorption band is observed with blueshifted wavelengths and high extinction coefficients (42000–44000 $M^{-1}cm^{-1}$). All of the absorption spectra are centered in the UV region and do not show drastic solvatochromism. Irradiation in the lower-energy absorption bands for most of the dyes listed in Table 1 leads to an intense emission band in the visible region with maxima ranging between 420 and 571 nm, quantum yields of 6–78%, and Stokes shifts of about 4500 cm^{-1} This is a significant improvement compared to previously reported non-extended HBO borate complexes, for which emission wavelengths were all located below 425 nm.[29]

In particular, compared to the unsubstituted HBO borate complex (see Scheme 1a, $\lambda_{abs}=349$ nm, $\lambda_{em}=401$ nm, $\Phi=26\%$ in CH_2Cl_2),[29] delocalization through an ethynyl spacer leads to a bathochromic shift in absorption and emission regardless of the position at which the fragment is connected to the HBO core (3, 4, or 5) or its electronic nature. Exten-

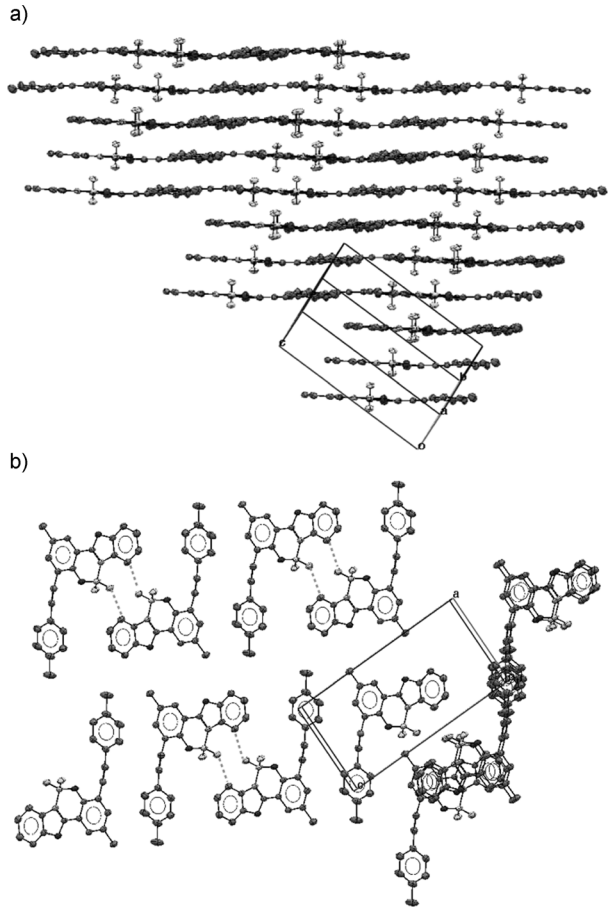

Figure 6. a) A view showing the layered crystal structure of complex **29**. b) View perpendicular to the layers showing dimeric association (CH···F interactions as dotted lines) and also the infinite stacking of the benzyl groups at the origin of the unit cell on one side, and the HBO platforms on the other side, along the *b* axis of complex **29**.

Table 1. Optical data measured in solution.

Dye	λ_{abs} [nm]	ε_{max} [$M^{-1}cm^{-1}$]	λ_{em} [nm]	Δ [cm^{-1}])	Φ_f[a]	τ [ns]	Solvent
11	366	9200	427	3800	0.17	2.29	toluene
	365	9400	425	4000	0.31	2.34	CH_2Cl_2
12	376	10000	445	4100	0.25	2.47	toluene
	376	7800	452	4500	0.38	2.92	CH_2Cl_2
13	371	8300	432	3800	0.23		toluene
	365	9100	432	4200	0.25	2.73	CH_2Cl_2
14	347	43200	520	9600	0.17	9.31	toluene
	350	39400	–[b]	–[b]	–[b]	–[b]	CH_2Cl_2
	368	10000	437	4300	0.18	1.81	$CH_2Cl_2+HCl_{(g)}$
	347	43800	–[b]	–[b]	–[b]	–[b]	CH_3CN
15	372	21800	431	3900	0.30	1.65	toluene
	370	21400	436	4100	0.42	1.74	CH_2Cl_2
16	388	9600	473	4600	0.37	2.82	cyclohexane
	388	15200	493	5500	0.50	4.40	toluene
	395	11600	571	7800	0.18	3.73	CH_2Cl_2
	361	25800	419	3800	0.29	1.43	$CH_2Cl_2+HCl_{(g)}$
	342	48000	514	9800	0.06	0.94	CH_3CN
	382	13800	562	8400	0.09	4.03	THF
21	369	41900	421	3300	0.32	1.05	toluene
	371	43500	420	3100	0.53	1.00	CH_2Cl_2
22	390	33900	449	3400	0.78	1.25	toluene
	400	30100	512	5500	0.73	2.50	CH_2Cl_2
	345	29400	492	8700	0.24	1.98	$CH_2Cl_2+HCl_{(g)}$
	401	32500	553	6900	0.08	1.02	CH_3CN
	400	37900	506	5300	0.44	2.32	THF
29	388	14600	457	3900	0.31	2.97	toluene
	383	14100	457	4200	0.32	3.02	CH_2Cl_2
30	380	16700	444	3800	0.52	2.59	toluene
	373	19500	494	6600	0.18	6.31	CH_2Cl_2
	332	21400	373	3300	0.25	2.31	$CH_2Cl_2+HCl_{(g)}$
	379	18700	536	7700	0.11	5.68	CH_3CN
	387	16700	478	5700	0.40	4.44	THF
33	362	15000	513	8100	0.48	2.43	CH_2Cl_2
	503	63400	513	390	0.50		
36	416	78400	479	3200	0.20	0.46	CH_2Cl_2

[a] Quantum yields determined in solution with quinine sulfate as reference ($\Phi=0.55$ in 1 N H_2SO_4, $\lambda_{ex}=366$ nm) for dyes emitting below 480 nm and Rhodamine 6G as reference ($\Phi=0.88$ in ethanol, $\lambda_{ex}=488$ nm) for dyes emitting between 480 and 570 nm. [b] Nonfluorescent.

sion of the conjugation through linking of a trimethylsilylacetylene fragment at the 5-position leads to a bathochromic shift of 16 nm in absorption and 26 nm in emission with respect to the unsubstituted compound and a quantum yield of 31% in CH_2Cl_2 (**11**). Further extending the conjugation by connecting a phenylacetylene module increases the quantum yield and bathochromically shifts the emission of the resulting borate complexes. For example, connection of the electron-deficient *p*-cyanophenylacetylene fragment at the 5-position provides bathochromically shifted dye **13** ($\lambda_{abs}=365$ nm, $\lambda_{em}=432$ nm, $\Phi=25\%$ in CH_2Cl_2), while the presence of a *p*-tolylacetylene module in dye **12** leads to a redshift in both absorption (26 nm) and emission (51 nm) with an improved quantum yield (38%) compared to the unsubstituted HBO borate complex. Switching from a methyl to a strongly electron donating *p*-dibutylphenylamino group (**14**) leads to a completely different photophysical behavior. Dye **14** exhibit a main absorption band at 350 nm, but its fluorescence emission is entirely quenched in CH_2Cl_2, presumably due to strong internal charge transfer (ICT) occurring in the complex.[34] These results are in strong contrast to recently published similar BF_2 complexes, for which direct connection of a dimethylamino group at the 5-position of an HBO core results in bright orange fluorescence at 597 nm.[30a,b] To confirm the hypothesis of strong ICT in complex **14**, absorption and emission spectra were recorded in CH_2Cl_2 after bubbling HCl gas. Since ICT is no longer effective due to protonation of the *p*-dibutylphenylamino group, a bright blue emission can be seen by the naked eye ($\lambda_{abs}=368$ nm, $\lambda_{em}=437$ nm, $\Phi=18\%$). The absorption of protonated **14** undergoes both a bathochromic and hypochromic shift ($\lambda_{abs}=350$ nm, $\varepsilon=39400$ for **14** in CH_2Cl_2 vs. $\lambda_{abs}=368$ nm, $\varepsilon=10000$ for **14** in $CH_2Cl_2+HCl_{(g)}$). Note that **14** is also emissive in toluene but is quenched in CH_3CN.

Introduction of a neighboring methoxyl group in dyes **15** and **16** leads to significant changes in the photophysical properties. A weak blueshift in absorption and emission as well as a higher extinction coefficient is observed for **15** versus **12** [$\lambda_{abs}=370$ nm ($\varepsilon=21800\,M^{-1}cm^{-1}$), $\lambda_{em}=436$ nm for **15** in CH_2Cl_2 compared to $\lambda_{abs}=376$ nm ($\varepsilon=7800\,M^{-1}cm^{-1}$), $\lambda_{em}=452$ nm for **12**]. This blueshift is ob-

served in spite of the slight electronic differences of the terminal groups on the ethynyl fragments between **12** (Me) and **15** (*t*Bu). Like for the *p*-dibutylaminophenylacetylene derivatives, drastic changes are observed for **16** compared to **14**. Indeed, unlike **14**, emission of which was quenched in CH_2Cl_2, excitation of **16** at 395 nm leads to a bright yellow-orange emission centered at 571 nm with $\Phi = 18\,\%$ (Figure 7). A pronounced hypsochromic shift of 152 nm

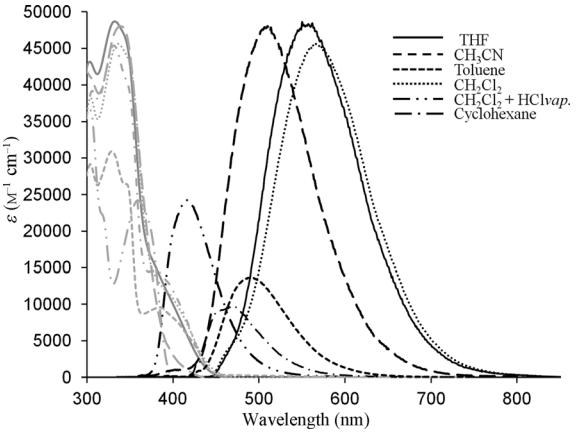

Figure 7. Absorption (gray) and fluorescence emission (black) spectra of HBO borate complex **16** in various solvents at room temperature.

occurs when HCl gas is bubbled through the solution ($\lambda_{em} =$ 419 nm) with an improved quantum yield of 29 %. Under these conditions, the solution remains homogeneous without precipitation of the salt. Furthermore, as seen in Figure 7, the fluorescence emission of **16** is solvatochromic and ranges from 473 nm in cyclohexane to 571 nm in CH_2Cl_2. This behavior seems consistent with pronounced ICT, but the value observed in CH_3CN is unexpected and not yet fully understood. The absorption of **16** is centered around 380 nm and does not undergo solvatochromism.

The absorption and emission spectra of the *p*-tolylacetylene regioisomers **12**, **21**, and **29** in CH_2Cl_2 are shown in Figure 8. Complexes **12** and **29** bearing a *p*-tolylacetylene

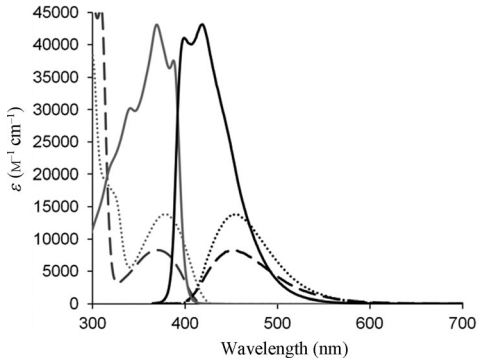

Figure 8. Absorption (gray) and fluorescence emission (black) spectra of HBO borate complexes **12** (5-isomer, – – –), **21** (4-isomer, ——) and **29** (3-isomer, ·····) in CH_2Cl_2 at room temperature.

fragment in the 5- and 3-position, respectively, exhibit similar photophysical characteristics, such as a large, unstructured absorption band ($\lambda_{abs} = 376$ nm for **12** and 383 nm for **29**) and a symmetrical emission band ($\lambda_{em} = 452$ nm for **12** with $\Phi = 38\,\%$ and $\lambda_{em} = 457$ nm for **29** with $\Phi = 32\,\%$). Their emission is mildly to nonsolvatochromic, consistent with weak ICT. In strong contrast, complex **21** exhibits structured, narrow, blueshifted absorption bands with increased extinction coefficients (around $45\,000\,M^{-1}cm^{-1}$). The emission bands fairly mirror the absorption bands and feature reduced Stokes shift (around $3000\,cm^{-1}$), consistent with a weakly polarized excited state. These experimental observations are indicative of a singlet-state emission with a significant internal cyanine character.[11]

The photophysical data of *p*-dibutylaminophenylacetylene complexes **14**, **16**, **22**, and **30** in CH_2Cl_2 are compiled in Figure 9. Complex **14**, which is not emissive in CH_2Cl_2, lights up in the presence of protons, a feature that is clearly

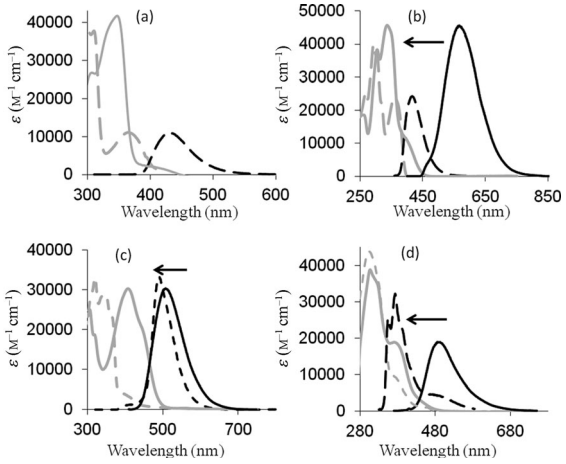

Figure 9. Absorption (gray) and fluorescence emission (black) spectra of HBO borate complexes a) **14**, b) **16**, c) **22**, and d) **30** in CH_2Cl_2 before (——) and after (– – –) bubbling HCl gas at room temperature.

indicative of pronounced ICT along the main molecular axis (Figure 9a). In complex **16**, the presence of a methoxy group in *ortho* position seems to prevent some of the nonradiative deactivation channels occurring, as highlighted by bright yellow-orange fluorescence in CH_2Cl_2. A strong hypsochromic shift in absorption and emission is observed after bubbling HCl *gas* through the solution (Figure 9b). The 4-regioisomer complex **22** exhibits bright green-yellow fluorescence at 512 nm with $\Phi = 72\,\%$ (Figure 9c). Protonation with HCl gas leads to a mild blueshift of 20 nm compared to the other regioisomers with a significant decrease in quantum yield (24 %). These experimental observations are consistent with the photophysical behavior of **21** and are indicative of a weakly polarized excited state for complexes substituted at the 4-position. Note that the absorption of protonated **22** undergoes a pronounced hypsochromic shift ($\lambda_{abs} =$ 400 nm in CH_2Cl_2 vs. $\lambda_{abs} = 345$ nm in $CH_2Cl_2 + HCl_{(g)}$). The 3-regioisomer **30** exhibits rather similar photophysical prop-

erties to those of complex **16** (Figure 9d) with an unstructured emission at 373 nm in CH_2Cl_2 and a broad emission band centered at 494 nm ($\Phi = 18\,\%$). Protonation with HCl gas leads to a significant hypsochromic shift and an increase of the quantum yield ($\lambda_{abs} = 332$ nm, $\lambda_{em} = 373$ nm, $\Phi = 25\,\%$). These results are suggestive of weaker ICT than those occurring in complexes **14** and **16**.

The absorption spectrum of mixed dyad **33** is a linear combination of those of the individual subunits, likely due to the orthogonality of the BODIPY and the HBO borate fragments (Figure 10), which is responsible for the weak

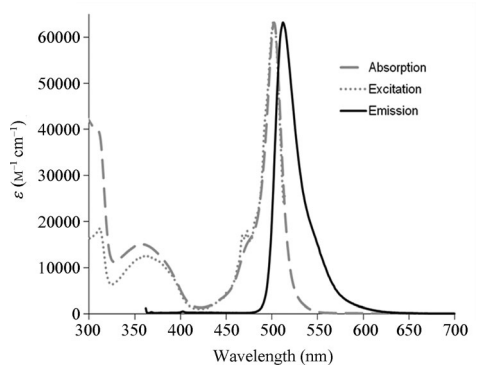

Figure 10. Absorption (dashed gray), excitation (dotted gray) and emission (black) of the BODIPY-HBO borate dyad **33**, in CH_2Cl_2 at room temperature.

conjugation between the two modules. Excitation in the lowest-energy band of the HBO module (349 nm) leads to sole emission of the BODIPY fluorophore in CH_2Cl_2 ($\lambda_{em} = 513$ nm, $\Phi = 48\,\%$). Note that no residual emission of the HBO borate fragment is observed, which suggests efficient energy transfer from the HBO borate complex to the BODIPY residue. This favorable situation is a consequence of the pronounced spectral overlap between the emission of the HBO and the absorption of the second excited state of the BODIPY fragment. Similar behavior was previously observed with pyrene or perylene as input energy source.[35]

Finally, mixed dyad **36** exhibits two absorption bands centered at 301 and 416 nm with a high extinction coefficient of around 80000 $M^{-1}cm^{-1}$ (Figure 11). Excitation in the lowest-energy band leads to a unique structured emission band at 479 nm with a quantum yield of 20%.

In order to correlate the photophysics with the strong π stacking observed in the X-ray structures (Figure 5 and 6), the solid-state luminescence properties of borate complexes **21** and **29** were investigated. Indeed, as shown in Figure 12, these complexes exhibit bright luminescence visible to the naked eye in the solid state under a 365 nm UV lamp, both as amorphous powders and as crystals (Figure 12). The highly crystalline powders were dispersed in KBr pellets ($\approx 10^{-6}$ M) and their emission and excitation spectra recorded (Figure 13). Additionally, the emission profile of single crystals were recorded by using an optical fiber connected to a spectrometer (Figure 13). The emission-band profiles of **21**

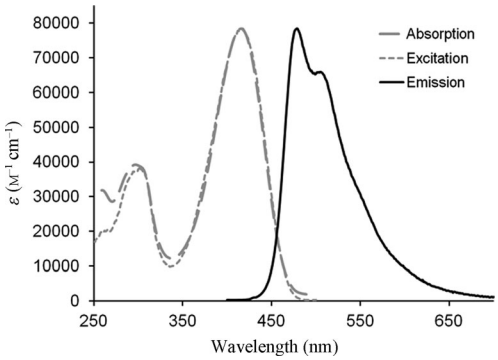

Figure 11. Absorption (dashed gray), excitation (dotted gray), and emission (black) of Boranil–HBO borate dyad **36** in CH_2Cl_2 at room temperature.

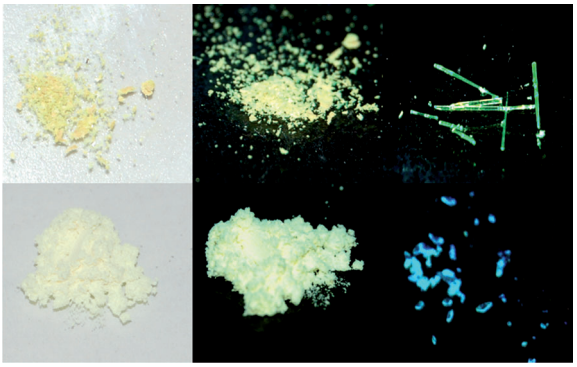

Figure 12. Photographs of borate complexes **21** (top) and **29** (bottom) as amorphous powders (left), amorphous powders under bench UV lamp (irradiation $\lambda_{ex} = 365$ nm; middle), and crystals under UV lamp ($\lambda_{ex} = 365$ nm; right).

and **29** are very similar, for example, an unstructured emission band at 491 and 464 nm, respectively. These represent redshifts of 2900 and 330 cm^{-1} compared to their emission-maximum wavelengths in CH_2Cl_2. The emission recorded on single crystals matches well that recorded on the powders for **21** and **29**. Their quantum yields, calculated from a spectrometer fitted with an integrating sphere, were found to be $\Phi = 29\,\%$ for **21** and $\Phi = 31\,\%$ for **29**. Excitation spectra were recorded with an emission wavelength set to the maximum of emission ($\lambda_{ex} = 411$ nm for **21** and 419 nm for **29**). Polyexponential decays were observed, presumably due to the presence of numerous aggregates with average lifetimes of 5.5 ns for **21** and 4.9 ns for **29**.

Solid-state luminescence usually arises from luminescent dyes carrying peripheral bulky groups that prevent close packing and subsequent aggregation-induced fluorescence annihilation.[16] On the other hand, aggregation-induced fluorescence is sometimes observed for dyes due to the restriction of intramolecular rotation in the solid state compared to solution.[36] The substituent groups and planarity of π-conjugated dyes play a pivotal role in the crystal packing and hence in the solid-state fluorescence properties. Some experimental studies provided evidence for solid-state emission properties correlated to tight packing in π-conjugated sys-

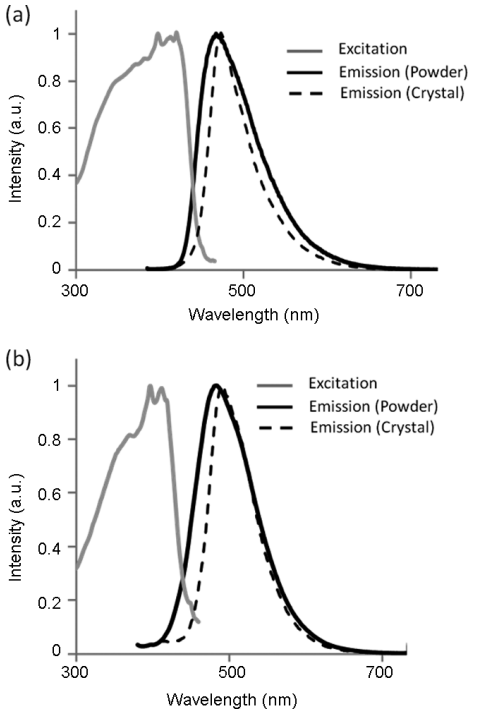

Figure 13. Solid-state excitation (gray) and emission recorded on powder dispersed in KBr pellets (black, continuous) or as crystals (black, dotted) of HBO borate complexes a) **21** and b) **29** at room temperature.

tems.[37] This is the case for complexes **21** and **29**, which are characterized by strong packing, governed by π–π interactions with interlayer distances of 3.18 and 3.22 Å, respectively. The redshifted emission is probably due to the formation of dimers in which the transition dipoles are arranged either in-line or in an oblique manner.[38]

Conclusion

We have synthesized three families of regioisomers of HBO borate complexes extended on the phenolate side by an ethynyl fragment at the 3-, 4-, or 5-position. Different photophysical properties were measured depending on the electronic nature of the ethynyl module and the position of connection to the HBO core. The 5- and 3-regioisomeric complexes display mild to strong ICT, especially for those including a *p*-dibutylaminophenylacetylene group in their structure. The emission band, which is strongly solvatochromic, is significantly blueshifted on protonation of the amino group in CH_2Cl_2. The 4-isomers display mildly solvatochromic singlet excited-state fluorescence. Moreover, these complexes exhibit fluorescence in the solid state, whereby the emission can be correlated to tight packing of the π-conjugated dyes. Finally, these novel fluorescent modules were attached to other photoactive subunits such as BODIPY, and strong energy transfer was observed due to favorable spectral overlap between the emission of the HBO fragment and the absorption of the BODIPY subunit. Further work will be directed to solubilizing these dyes in buffer solutions, a prerequisite for their conjugation to biomacromolecules such as enzymes or DNA.

Experimental Section

General methods and equipment: All reactions were performed under a dry atmosphere of argon by using standard Schlenk techniques. All chemicals were received from commercial sources (Aldrich, Alfa Aesar) and used without further purification. Dichloromethane was distilled over P_2O_5 under an argon atmosphere. Thin-layer chromatography (TLC) was performed on silica gel or aluminum oxide plates coated with fluorescent indicator. Chromatographic purifications were conducted with 40–63 μm silica gel or basic aluminum oxide. All mixtures of solvents are given in v/v ratio. The 200 (^{1}H), 300 (^{1}H), 400 (^{1}H), 50.3 (^{13}C), 75.46 (^{13}C), and 100.3 MHz (^{13}C) NMR spectra were recorded at room temperature with perdeuterated solvents and residual protonated solvent signals as internal references. The 128 MHz (^{11}B) NMR spectra were recorded at room temperature with borosilicate glass as reference. Mass spectra were measured with a ESI-MS mass spectrometer. Electronic absorption and emission spectra were measured under ambient conditions on commercial instruments. UV/Vis spectra were recorded on a dual-beam grating spectrophotometer with a 1 cm quartz cell. Fluorescence spectra were recorded with a spectrofluorimeter. Solvents for spectroscopy were of spectroscopic grade and used as received. All fluorescence spectra were corrected. Luminescence lifetimes were measured on a spectrofluorimeter by using software in time-correlated single-photon mode coupled to a stroboscopic system. The excitation source was a laser diode ($\lambda = 320$ nm). The instrument response function was determined by using a light-scattering solution (LUDOX). The fluorescence quantum yield (Φ_{exp}) was calculated from Equation (1).

$$\Phi_{exp} = \Phi_{ref} \frac{I}{I_{ref}} \frac{OD_{ref}}{OD} \frac{\eta^2}{\eta_{ref}^2} \quad (1)$$

where I denotes the integral of the corrected emission spectrum, OD the optical density at the excitation wavelength, and η the refractive index of the medium. The reference systems used were: quinine, $\Phi = 55\,\%$ in H_2SO_4 1 N, $\lambda_{ex} = 366$ nm for dyes emitting below 480 nm; Rhodamine 6G, $\Phi = 88\,\%$ in ethanol, $\lambda_{ex} = 488$ nm for dyes emitting between 480 and 570 nm; and cresyl violet, $\Phi = 55\,\%$ $\lambda_{ex} = 546$ nm in ethanol for dyes emitting above 570 nm.

Synthesis: All reagents were used directly as obtained commercially unless otherwise noted. 2-Hydroxy-5-iodobenzaldehyde (**1**),[39] 4-ethynylbenzonitrile,[40] *p*-(dibutylamino)phenylacetylene,[41] BODIPY (**31**),[42] and Boranil (**34**)[31a] were synthesized according to reported procedures. Synthetic protocols for the preparation of salicylaldehydes **2**, **17**, and **23** and 2-(2′-hydroxyphenyl)benzoxazoles (HBOs) **3**–**10**, **18**–**20**, and **24**–**28** can be found in the Supporting Information.

General procedure for the synthesis of HBO borate complexes: $BF_3{\cdot}Et_2O$ (6 equiv) was added by syringed to a stirred solution of the corresponding HBO in freshly distilled dichloromethane (0.1 mL mg^{-1}) under argon. After 5 min, *N*,*N*-diisopropylethylamine (DIEA, 6 equiv) was added and the resulting mixture stirred at room temperature for 1 h. The crude solution was then filtered through a column of basic Al_2O_3, eluted with CH_2Cl_2, and the solvents were evaporated in vacuo. Pure HBO borate complexes were obtained as white to yellow powders after recrystallization from pentane or cyclohexane.

HBO borate complex 11: Beige powder. 75 %. ^{1}H NMR (300 MHz, $CDCl_3$): $\delta = 8.10$ (m, 1H, CH Ar), 7.97–8.00 (m, 1H, CH Ar), 7.70–7.76 (m, 2H, CH Ar), 7.59–7.62 (m, 2H, CH Ar), 7.18 (d, 1H, CH Ar, $J =$ 8.7 Hz), 0.27 ppm (s, 9H, CH_3); ^{13}C NMR (75.4 MHz, $CDCl_3$): $\delta = 159.5$, 149.0, 141.1, 130.7, 129.2, 128.3, 127.9, 127.7, 120.6, 117.2, 115.7, 111.8, 106.9, 103.0, 94.8, 0.0 ppm; ^{11}B NMR (128.38 MHz, $CDCl_3$): $\delta = 1.38$ ppm (br s); elemental analysis (%) calcd for $C_{18}H_{16}BF_2NO_2Si$: C 60.86, H 4.54,

N 3.94; found: C 60.74, H 4.84, N 3.70; EI-MS: *m/z* (%): 355.0 (100), 336.0 (25).

HBO borate complex 12: White powder. 92%. ^{1}H NMR (300 MHz, $CDCl_3$): δ = 8.14 (d, 1H, CH Ar, J = 2.1 Hz), 7.98–8.01 (m, 1H, CH Ar), 7.73–7.79 (m, 2H, CH Ar), 7.57–7.64 (m, 2H, CH Ar), 7.44 (d, 2H, CH Ar, J = 8.1 Hz), 7.23 (d, 1H, CH Ar, J = 8.7 Hz), 7.18 (d, 2H, CH Ar, J = 7.8 Hz), 2.39 ppm (s, 3H, CH_3); ^{13}C NMR (75.4 MHz, $CDCl_3$): δ = 166.7, 159.2, 148.9, 140.7, 138.8, 131.5, 130.7, 129.2, 128.4, 127.8, 127.6, 120.6, 119.7, 117.2, 116.0, 111.8, 106.2, 89.8, 86.8, 21.6 ppm; ^{11}B NMR (128.38 MHz, $CDCl_3$): δ = 1.43 ppm (brs); elemental analysis (%) calcd for $C_{22}H_{14}BF_2NO_2$: C 70.81, H 3.78, N 3.75; found: C 70.57, H 3.59, N 3.66; EI-MS: *m/z* (%): 373.1 (100), 354.0 (35).

HBO borate complex 13: Beige powder. 79%. ^{1}H NMR (300 MHz, $CDCl_3$): δ = 8.18–8.19 (m, 1H, CH Ar), 7.98–8.02 (m, 1H, CH Ar), 7.75–7.81 (m, 2H, CH Ar), 7.56–7.68 (m, 6H, CH Ar), 7.24–7.25 ppm (m, 1H, CH Ar); ^{13}C NMR (100 MHz, $CDCl_3$): δ = 160.9, 159.8, 148.9, 140.7, 132.2, 132.1, 132.1, 130.6, 129.1, 128.0, 127.8, 127.8, 120.9, 118.5, 117.3, 114.7, 111.8, 106.4, 91.8, 88.0 ppm; ^{11}B NMR (128.38 MHz, $CDCl_3$): δ = 1.38 ppm (brs); elemental analysis (%) calcd for $C_{22}H_{11}BF_2N_2O_2$: C 68.79, H 2.89, N 7.29; found: C 69.18, H 2.72, N 6.93; EI-MS: *m/z* (%): 384.0 (100), 365.1 (10).

HBO borate complex 14: Yellow powder. 75%. ^{1}H NMR (300 MHz, $CDCl_3$): δ = 8.10 (d, 1H, CH Ar, J = 1.5 Hz), 7.97–8.00 (m, 1H, CH Ar), 7.73–7.77 (m, 2H, CH Ar), 7.58–7.62 (m, 2H, CH Ar), 7.37 (d, 2H, CH Ar, J = 9 Hz), 7.20 (d, 1H, CH Ar, J = 9 Hz), 6.59 (d, 2H, CH Ar, J = 8.4 Hz), 3.29 (t, 4H, CH_2, J = 7.8 Hz), 1.52–1.63 (m, 4H, CH_2), 1.33–1.40 (m, 4H, CH_2), 0.97 ppm (t, 6H, CH_3, J = 7.5 Hz); ^{13}C NMR (100 MHz, $CDCl_3$): δ = 161.4, 158.8, 149.0, 140.7, 133.1, 132.9, 130.8, 127.9, 127.7, 127.6, 120.5, 117.2, 111.8, 111.3, 108.1, 106.1, 91.2, 85.3, 50.8, 29.4, 20.3, 14.0 ppm; ^{11}B NMR (128.38 MHz, $CDCl_3$): δ = 1.41 ppm (brs); elemental analysis (%) calcd for $C_{29}H_{29}BF_2N_2O_2$: C 71.62, H 6.01, N 5.76; found: C 71.44, H 5.69, N 5.49; EI-MS: *m/z* (%): 486.1 (100).

HBO borate complex 15: Off-white powder. 83%. ^{1}H NMR (300 MHz, $CDCl_3$): δ = 8.07 (s, 1H, CH Ar), 7.90–7.93 (m, 1H, CH Ar), 7.68–7.71 (m, 1H, CH Ar), 7.52–7.59 (m, 2H, CH Ar), 7.50 (d, 2H, CH Ar, J = 8.7 Hz), 7.39 (d, 2H, CH Ar, J = 8.4 Hz), 6.70 (s, 1H, CH Ar, J = 8.4 Hz), 3.99 (s, 3H, CH_3), 1.34 ppm (s, 9H, CH_3); ^{13}C NMR (100 MHz, $CDCl_3$): δ = 167.4, 161.8, 151.8, 148.7, 131.4, 130.8, 130.2, 127.3, 127.0, 125.4, 120.0, 116.6, 111.6, 107.7, 101.5, 99.1, 93.5, 82.9, 56.6, 34.9, 31.2 ppm; ^{11}B NMR (128.38 MHz, $CDCl_3$): δ = 1.38 ppm (brs); elemental analysis (%) calcd for $C_{26}H_{22}BF_2NO_3$: C 70.13, H 4.98, N 3.15; found: C 70.39, H 5.28, N 3.37; EI-MS: *m/z* (%): 445.1 (100), 426.2 (15).

HBO borate complex 16: Yellow powder. 88%. ^{1}H NMR (300 MHz, $CDCl_3$): δ = 8.03 (s, 1H, CH Ar), 7.89–7.92 (m, 1H, CH Ar), 7.67–7.70 (m, 1H, CH Ar), 7.51–7.55 (m, 2H, CH Ar), 7.39 (d, 2H, CH Ar, J = 8.7 Hz), 6.67 (s, 1H, CH Ar), 6.58 (d, 2H, CH Ar, J = 9 Hz), 3.98 (s, 3H, CH_3), 3.29 (t, 4H, CH_2, J = 7.8 Hz), 1.53–1.64 (m, 4H, CH_2), 1.30–1.43 (m, 4H, CH_2), 0.97 ppm (t, 6H, CH_3, J = 7.2 Hz); ^{13}C NMR (75.4 MHz, $CDCl_3$): δ = 167.3, 161.4, 148.7, 148.1, 132.9, 130.8, 129.5, 127.2, 126.9, 116.5, 111.5, 111.2, 108.6, 108.4, 101.4, 99.0, 94.9, 81.1, 56.5, 50.7, 29.4, 20.3, 14.0 ppm; ^{11}B NMR (128.38 MHz, $CDCl_3$): δ = 1.40 ppm; elemental analysis (%) calcd for $C_{30}H_{31}BF_2N_2O_3$: C 69.78, H 6.05, N 5.42; found: C 69.57, H 5.75, N 5.18; EI-MS: *m/z* (%): 516.1 (100), 497.1 (35).

HBO borate complex 21: Yellow powder. 65%. ^{1}H NMR (300 MHz, $CDCl_3$): δ = 7.97–8.00 (m, 1H, CH Ar), 7.92 (d, 1H, CH Ar, J = 8.1 Hz), 7.71–7.77 (m, 1H, CH Ar), 7.54–7.63 (m, 2H, CH Ar), 7.47 (d, 2H, CH Ar, J = 8.4 Hz), 7.46 (d, 1H, CH Ar, J = 1.5 Hz), 7.18–7.23 (m, 3H, CH Ar), 2.39 ppm (s, 3H, CH_3); ^{13}C NMR (75.4 MHz, $CDCl_3$): δ = 159.3, 148.9, 139.6, 133.3, 131.9, 130.8, 129.3, 127.6, 127.6, 125.4, 123.6, 122.7, 119.2, 117.1, 111.7, 105.4, 95.1, 87.9, 21.6 ppm; ^{11}B NMR (128.38 MHz, $CDCl_3$): δ = 1.39 ppm (brs); elemental analysis (%) calcd for $C_{22}H_{14}BF_2NO_2$: C 70.81, H 3.78, N 3.75; found: C 70.54, H 3.52, N 3.52; EI-MS: *m/z* (%): 373.0 (100), 354.1 (30).

HBO borate complex 22: Orange powder. 75%. ^{1}H NMR (300 MHz, $CDCl_3$): δ = 7.85–7.88 (m, 1H, CH Ar), 7.76 (d, 1H, CH Ar, J = 8.4 Hz), 7.61–7.64 (m, 1H, CH Ar), 7.43–7.50 (m, 2H, CH Ar), 7.30 (d, 2H, CH Ar, J = 9 Hz), 7.19 (d, 1H, CH Ar, J = 4.8 Hz), 7.05 (d, 1H, CH Ar, J = 8.4 Hz), 6.50 (d, 2H, J = 9 Hz), 3.22 (t, 4H, CH_2, J = 8.1 Hz), 1.45–1.56 (m, 4H, CH_2), 1.23–1.35 (m, 4H, CH_2), 0.89 ppm (t, 6H, CH_3, J = 7.2 Hz); ^{13}C NMR (75.4 MHz, $CDCl_3$): δ = 161.4, 159.3, 148.9, 148.6, 134.4, 133.5, 130.9, 127.4, 127.4, 125.3, 123.4, 121.8, 116.9, 111.7, 111.3, 107.5, 104.5, 97.7, 87.3, 50.8, 29.4, 20.4, 14.0 ppm; elemental analysis (%) calcd for $C_{29}H_{29}BF_2N_2O_2$: C 71.62, H 6.01, N 5.76; found: C 71.42, H 5.84, N 5.42; EI-MS: *m/z* (%): 486.1 (100), 467.1 (20).

HBO borate complex 29: Yellow powder. 88%. ^{1}H NMR (300 MHz, $CDCl_3$): δ = 7.98–8.01 (s, 1H, CH Ar), 7.71–7.74 (m, 1H, CH Ar), 7.67 (d, 2H, CH Ar, J = 10.2 Hz), 7.55–7.58 (m, 2H, CH Ar), 7.51 (d, 2H, CH Ar, J = 8.1 Hz), 7.17 (d, 2H, J = 7.8 Hz), 2.38 ppm (s, 6H, CH_3); ^{13}C NMR (75.4 MHz, $CDCl_3$): δ = 161.7, 158.0, 149.0, 142.0, 138.6, 131.8, 130.8, 129.6, 129.1, 127.6, 127.5, 124.7, 120.2, 117.2, 115.8, 111.7, 115.8, 111.7, 105.9, 95.4, 83.7, 21.6, 20.3 ppm; elemental analysis (%) calcd for $C_{23}H_{16}BF_2NO_2$: C 71.35, H 4.17, N 3.62; found: C 71.28, H 4.04, N 3.58; EI-MS: *m/z* (%): 387.1 (100), 368.1(25).

HBO borate complex 30: Yellow powder. 71%. ^{1}H NMR (300 MHz, $CDCl_3$): δ = 7.97 (d, 1H, CH Ar, J = 1.8 Hz), 7.69–7.72 (m, 1H, CH Ar), 7.53–7.60 (m, 4H, CH Ar), 7.44 (d, 2H, CH Ar, J = 6.6 Hz), 6.60 (d, 2H, CH Ar, J = 6.9 Hz), 3.29 (t, 4H, CH_2, J = 5.7 Hz), 2.34 (s, 3H, CH_3), 1.55–1.62 (m, 4H, CH_2), 1.32–1.42 (m, 4H, CH_2), 0.97 ppm (t, 6H, CH_3, J = 5.4 Hz); ^{13}C NMR (75.4 MHz, $CDCl_3$): δ = 161.8, 157.7, 149.0, 141.5, 133.3, 130.8, 129.5, 127.5, 127.4, 123.8, 117.0, 116.5, 111.7, 111.4, 111.4, 105.7, 96.9, 82.3, 50.9, 29.4, 20.4, 14.0 ppm; ^{11}B NMR (128.38 MHz, $CDCl_3$): δ = 1.54 ppm (brs); elemental analysis (%) calcd for $C_{30}H_{31}BF_2N_2O_2$: C 72.01, H 6.24, N 5.60; found: C 71.65, H 5.92, N 5.54; EI-MS: *m/z* (%): 500.1 (100), 481.1(10).

HBO borate complex 33: Red powder. 83%. ^{1}H NMR (300 MHz, $CDCl_3$): δ = 8.20 (d, 1H, CH Ar, J = 2.1 Hz), 8.00–8.03 (m, 1H, CH Ar), 7.76–7.83 (m, 2H, CH Ar), 7.68 (d, 2H, CH Ar, J = 8.1 Hz), 7.61–7.64 (m, 2H, CH Ar), 7.32 (d, 2H, CH Ar, J = 8.1 Hz), 7.28 (s, 1H, CH Ar), 6.00 (s, 2H, CH Ar), 2.57 (s, 6H, CH_3), 1.45 ppm (s, 6H, CH_3); ^{13}C NMR (75.4 MHz, $CDCl_3$): δ = 161.0, 159.6, 155.9, 149.0, 143.0, 140.7, 135.3, 132.3, 131.2, 130.7, 129.1, 128.8, 128.4, 128.3, 128.0, 127.8, 123.7, 121.5, 120.9, 117.3, 115.3, 111.8, 106.4, 88.9, 31.0, 14.7 ppm; ^{11}B NMR (128.38 MHz, $CDCl_3$): δ = 1.45 ppm ($J_{B,F}$ = 6.4 Hz), 0.80 ($J_{B,F}$ = 31.9 Hz); elemental analysis (%) calcd for $C_{34}H_{25}B_2F_4N_3O_2$: C 67.48, H 4.16, N 6.94; found: C 67.22, H 3.83, N 6.77; EI-MS: *m/z* (%): 605.1 (100), 586.1(40), 567.2(10).

HBO borate complex 36: Yellow powder. 56%. ^{1}H NMR (200 MHz, $CDCl_3$): δ = 8.18(s, 1H, CH Ar) 8.03 (m, 2H, CH imine + CH Ar), 7.79 (m, 2H, CH Ar), 7.57 (m, 7H, CH Ar), 7.24 (m, 1H, CH Ar), 6.39 (d, 1H, J = 8.6 Hz, CH Ar), 6.26 (s, 1H, CH Ar) 3.47 (q, 4H, J = 7.0 Hz, CH_2), 1.25 ppm (t, 6H, J = 7.0 Hz, CH_3); ^{13}C NMR (75.4 MHz, $CDCl_3$): δ = 162.3, 157.8, 156.8, 149.2, 143.3, 140.9, 134.2, 132.8, 128.9, 128.1, 123.4, 122.3, 117.4, 112.0, 107.4, 107.2, 106.5, 98.4, 89.1, 88.9, 44.8, 12.9 ppm; elemental analysis (%) calcd for $C_{32}H_{25}B_2F_4N_3O_3$: C 64.36, H 4.22, N 7.04; found: C 64.09, H 3.92, N 6.82; EI-MS: *m/z* (%): 597.0 (100), 559.1(35).

Acknowledgements

We thank the Centre National de la Recherche Scientifique (CNRS) for financial support and the Ministère de l'Enseignement Supérieur et de la Recherche for a MENRT Ph.D. fellowship for D.F.

[1] a) B. N. G. Giepmans, S. R. Adams, M. H. Ellisman, R. Y. Tsien, *Science* **2006**, *312*, 217–224; b) M. Y. Berezin, S. Achilefu, *Chem. Rev.* **2010**, *110*, 2641–2684; c) H. Kobayashi, M. Ogawa, R. Alford, P. L. Choyke, Y. Urano, *Chem. Rev.* **2010**, *110*, 2620–2640; d) H. Kobayashi, P. L. Choyke, *Acc. Chem. Res.* **2011**, *44*, 83–90; e) J. M. Baumes, J. J. Gassensmith, J. Giblin, J.-J. Lee, A. G. White, W. J. Culligan, W. M. Leevy, M. Kuno, B. D. Smith, *Nat. Chem.* **2010**, *2*, 1025–1030.

[2] a) C. D. Entwistle, T. B. Marder, *Chem. Mater.* **2004**, *16*, 4574–4585; b) C. D. Entwistle, T. B. Marder, *Angew. Chem.* **2002**, *114*, 3051–3056; *Angew. Chem. Int. Ed.* **2002**, *41*, 2927–2931; c) K. Kalyanasun-

daram, M. Graetzel, *Curr. Opin. Biotechnol.* **2010**, *21*, 298–310; d) S. Qu, H. Tian, *Chem. Commun.* **2012**, *48*, 3039–3051.
[3] a) M. Schäferling, *Angew. Chem. Int. Ed.* **2012**, *51*, 3532–3554; b) N. Boens, V. Leen, W. Dehaen, *Chem. Soc. Rev.* **2012**, *41*, 1130–1172.
[4] M. S. T. Gonçalves, *Chem. Rev.* **2009**, *109*, 190–212.
[5] a) R. Jelinek, S. Kolusheva, *Chem. Rev.* **2004**, *104*, 5987–6015; b) J.-X. Wang, Q. Chen, N. Bian, F. Yang, J. Sun, A.-D. Qi, C.-G. Yan, B.-H. Han, *Org. Biomol. Chem.* **2011**, *9*, 2219–2226.
[6] Q. Chen, J.-X. Wang, F. Yang, D. Zhou, N. Bian, X.-J. Zhang, C.-G. Yan, B.-H. Han, *J. Mater. Chem.* **2011**, *21*, 13554–13560.
[7] U. H. F. Bunz, V. Rotello, *Angew. Chem.* **2010**, *122*, 3338–3350; *Angew. Chem. Int. Ed.* **2010**, *49*, 3268–3279.
[8] K. Welsher, Z. Liu, S. P. Sherlock, J. Tucker Robinson, Z. Chen, D. Daranciang, H. Dai, *Nat. Nanotechnol.* **2009**, *4*, 773–780.
[9] S. R. Trenor, A. R. Shultz, B. L. Love, T. E. Long, *Chem. Rev.* **2004**, *104*, 3059–3077.
[10] W. Shi, H. Ma, *Chem. Commun.* **2012**, *48*, 8732–8744.
[11] A. Mishra, R. K. Behera, P. K. Behera, B. K. Mishra, G. E. Behera, *Chem. Rev.* **2000**, *100*, 1973–2012.
[12] H. N. Kim, M. H. Lee, H. J. Kim, J. S. Kim, J. Yoon, *Chem. Soc. Rev.* **2008**, *37*, 1465–1472.
[13] a) D. T. Quang, J. S. Kim, *Chem. Rev.* **2010**, *110*, 6280–6301; b) H. S. Hewage, E. V. Anslyn, *J. Am. Chem. Soc.* **2009**, *131*, 13099–13106; c) S. Sreejith, P. Carol, P. Chithra, A. Ajayaghosh, *J. Mater. Chem.* **2008**, *18*, 264–274.
[14] a) A. Loudet, K. Burgess, *Chem. Rev.* **2007**, *107*, 4891–4932; b) G. Ulrich, R. Ziessel, A. Harriman, *Angew. Chem.* **2008**, *120*, 1202–1219; *Angew. Chem. Int. Ed.* **2008**, *47*, 1184–1207; c) R. Ziessel, G. Ulrich, A. Harriman, *New J. Chem.* **2007**, *31*, 496–501.
[15] J. F. Araneda, W. E. Piers, B. Heyne, M. Parvez, R. McDonald, *Angew. Chem.* **2011**, *123*, 12422–12425; *Angew. Chem. Int. Ed.* **2011**, *50*, 12214–12217.
[16] M. Shimizu, T. Hiyama, *Chem. Asian J.* **2010**, *5*, 1516–1531.
[17] a) T. Ozdemir, S. Atilgan, I. Kutuk, L. T. Yildirim, A. Tulek, M. Bayindir, E. U. Akkaya, *Org. Lett.* **2009**, *11*, 2105–2107; b) H. Lu, Q. Wang, L. Gai, Z. Li, Y. Deng, X. Xiao, G. Lai, Z. Shen, *Chem. Eur. J.* **2012**, *18*, 7852–7861.
[18] Y.-L. Rao, S. Wang, *Inorg. Chem.* **2011**, *50*, 12263–12274.
[19] a) Y. Yang, X. Su, C. N. Carroll, I. Aprahamian, *Chem. Sci.* **2012**, *3*, 610–613; b) Q. D. Liu, M. S. Mudadu, R. Thummel, Y. Tao, S. N. Wang, *Adv. Funct. Mater.* **2005**, *15*, 143–154; c) D. Suresh, C. S. B. Gomes, P. T. Gomes, R. E. Di Paolo, A. L. Maçanita, M. J. Calhorda, A. Charas, J. Morgado, M. T. Duarte, *Dalton Trans.* **2012**, *41*, 8502–8505; d) Y. Kubota, T. Tsuzuki, K. Funabiki, M. Ebihara, M. Matsui, *Org. Lett.* **2010**, *12*, 4010–4013; e) D. Curiel, M. Más-Montoya, L. Usea, A. Espinosa, R. A. Orenes, P. Molina, *Org. Lett.* **2012**, *14*, 3360–3363.
[20] a) H. Kim, A. Burghart, M. B. Welch, J. Reibenspies, K. Burgess, *Chem. Commun.* **1999**, 1889–1890; b) Y. Tomimori, T. Okujima, T. Yano, S. Mori, N. Ono, H. Yamada, H. Uno, *Tetrahedron* **2011**, *67*, 3187–3193; c) Y. Kubo, Y. Minowa, T. Shoda, K. Takeshita, *Tetrahedron Lett.* **2010**, *51*, 1600–1602; d) A. Loudet, R. Bandichhor, K. Burgess, A. Palma, S. O. McDonnell, M. J. Hall, D. F. O'Shea, *Org. Lett.* **2008**, *10*, 4771–4774.
[21] a) F. Montalbano, N. R. Candeias, L. F. Veiros, V. André, M. T. Duarte, M. R. Bronze, R. Moreira, P. M. P. Gois, *Org. Lett.* **2012**, *14*, 988–994; b) H. Zhang, C. Huo, K. Ye, P. Zhang, W. Tian, Y. Wang, *Inorg. Chem.* **2006**, *45*, 2788–2794; c) H. Zhang, C. Huo, J. Zhang, P. Zhang, W. Tian, Y. Wang, *Chem. Commun.* **2006**, 281–283.
[22] a) Z. Zhang, H. Bi, Y. Zhang, D. Yao, H. Gao, Y. Fan, H. Zhang, Y. Wang, Y. Wang, Z. Chen, D. Ma, *Inorg. Chem.* **2009**, *48*, 7230–7236; b) Y. Cui, S. Wang, *J. Org. Chem.* **2006**, *71*, 6485–6496; c) Y. Zhou, Y. Xiao, S. Chi, X. Qian, *Org. Lett.* **2008**, *10*, 633–636.
[23] Y. Zhou, J. W. Kim, M. J. Kim, W.-J. Son, S. J. Han, H. N. Kim, S. Han, Y. Kim, C. Lee, S.-J. Kim, D. H. Kim, J.-J. Kim, J. Yoon, *Org. Lett.* **2010**, *12*, 1272–1275.
[24] J. Feng, B. Liang, D. Wang, L. Xue, X. Li, *Org. Lett.* **2008**, *10*, 4437–4440.
[25] Y.-K. Lim, S. Wallace, J. C. Bollinger, X. Chen, D. Lee, *Inorg. Chem.* **2007**, *46*, 1694–1703.
[26] a) Y. Kubota, H. Hara, S. Tanaka, K. Funabiki, M. Matsui, *Org. Lett.* **2011**, *13*, 6544–6547; b) Y. Kubota, S. Tanaka, K. Funabiki, M. Matsui, *Org. Lett.* **2012**, *14*, 4682–4685.
[27] D. P. Murale, K. M. Lee, K. Kim, D. G. Churchill, *Chem. Commun.* **2011**, *47*, 12512–12514.
[28] M. J. Kwak, Y. Kim, *Bull. Korean Chem. Soc.* **2009**, *30*, 2865–2866.
[29] J. Massue, D. Frath, P. Retailleau, G. Ulrich, R. Ziessel, *Org. Lett.* **2012**, *14*, 230–233.
[30] a) D. Li, H. Zhang, C. Wang, S. Huang, J. Guo, Y. Wang, *J. Mater. Chem.* **2012**, *22*, 4319–4328; b) M. Santra, H. Moon, M.-H. Park, T.-W. Lee, Y. K. Kim, K. H. Ahn, *Chem. Eur. J.* **2012**, *18*, 9886–9893; c) D. Li, K. Wang, S. Huang, S. Qu, X. Liu, Q. Zhu, H. Zhang, Y. Wang, *J. Mater. Chem.* **2011**, *21*, 15298–15304.
[31] a) D. Frath, S. Azizi, P. Retailleau, G. Ulrich, R. Ziessel, *Org. Lett.* **2011**, *13*, 3414–3417; b) D. Frath, S. Azizi, G. Ulrich, R. Ziessel, *Org. Lett.* **2012**, *14*, 4774–4777.
[32] T. Iijima, A. Momotake, Y. Shinohara, T. Sato, Y. Nishimura, T. Arai, *J. Phys. Chem. A* **2010**, *114*, 1603–1609 and references cited therein.
[33] a) Y.-Y. Sun, J.-H. Liao, J.-M. Fang, P.-T. Chou, C.-H. Shen, C.-W. Hsu, L.-C. Chen, *Org. Lett.* **2006**, *8*, 3713–3716; b) J. Massue, G. Ulrich, R. Ziessel, unpublished results.
[34] L. Bonardi, G. Ulrich, R. Ziessel, *Org. Lett.* **2008**, *10*, 2183–2186.
[35] A. Harriman, G. Izzet, R. Ziessel, *J. Am. Chem. Soc.* **2006**, *128*, 10868–10875.
[36] a) Y. Hong, J. W. Y. lam, B. Z. Tang, *Chem. Commun.* **2009**, 4232–4253; b) R. Hu, C. F. A. Gómez-Durán, J. W. Yip Lam, J. L. Belmonte-Vázquez, C. Deng, S. Chen, R. Ye, E. Pena-Cabrera, Y. Zhong, K. S. Wong, B. Z. Tang, *Chem. Commun.* **2012**, *48*, 10099–10101.
[37] a) H. Langhals, T. Potrawa, H. Nöth, G. Linti, *Angew. Chem.* **1989**, *101*, 497–499; *Angew. Chem. Int. Ed. Engl.* **1989**, *28*, 478–480; b) J. Cornil, D. Beljonne, J.-P. Calbert, J.-L. Brédas, *Adv. Mater.* **2001**, *13*, 1053–1067; c) J. Massin, W. Dayoub, J.-C. Mulatier, C. Aronica, Y. Bretonnière, C. Andraud, *Chem. Mater.* **2011**, *23*, 862–873; d) A. D'Aléo, D. Gachet, V. Heresanu, M. Giorgi, F. Fages, *Chem. Eur. J.* **2012**, *18*, 12764–12772.
[38] a) M. Kasha, H. R. Rawls, M. A. El-Bayoumi, *Pure Appl. Chem.* **1965**, *11*, 371–392; b) M. Shimizu, R. Kaki, Y. Takeda, T. Hiyama, N. Nagai, H. Yamagishi, H. Furutani, *Angew. Chem. Int. Ed.* **2012**, *51*, 4095–4099.
[39] Y. M. Choi-Sledeski, D. G. McGarry, D. M. Green, H. J. Mason, M. R. Becker, R. S. Davis, W. R. Ewing, W. P. Dankulich, V. E. Manetta, R. L. Morris, A. P. Spada, D. L. Cheney, K. D. Brown, D. J. Colussi, V. Chu, C. L. Heran, S. R. Morgan, R. G. Bentley, R. J. Leadley, S. Maignan, J.-P. Guilloteau, C. T. Dunwiddie, H. W. Pauls, *J. Med. Chem.* **1999**, *42*, 3572–3587.
[40] C. Richardson, C. A. Reed, *J. Org. Chem.* **2007**, *72*, 4750–4755.
[41] J. J. Miller, J. A. Marsden, M. M. Haley, *Synlett* **2004**, *1*, 165–168.
[42] Z. Li, R. Bittman, *J. Org. Chem.* **2007**, *72*, 8376–8382.

Received: October 10, 2012
Revised: December 18, 2012
Published online: February 27, 2013

